JOC Article

Nitroxide Bound β-Cyclodextrin: Is There an Inclusion Complex?

David Bardelang,[†] Antal Rockenbauer,*[,‡] Laszlo Jicsinszky,[§] Jean-Pierre Finet,*[,†] Hakim Karoui,[†] Sandrine Lambert,[†] Sylvain R. A. Marque,[†] and Paul Tordo[†]

UMR 6517 CNRS et Aix-Marseille Université, Avenue Escadrille Normandie-Niemen, Marseille 13397, France, Chemical Research Center, Institute of Structural Chemistry, P.O. Box 17, H-125 Budapest, Hungary, and Cyclolab Ltd., P.O. Box 435, H-1525 Budapest, Hungary

jean-pierre.finet@up.univ-mrs.fr; rocky@chemres.hu

Received June 9, 2006

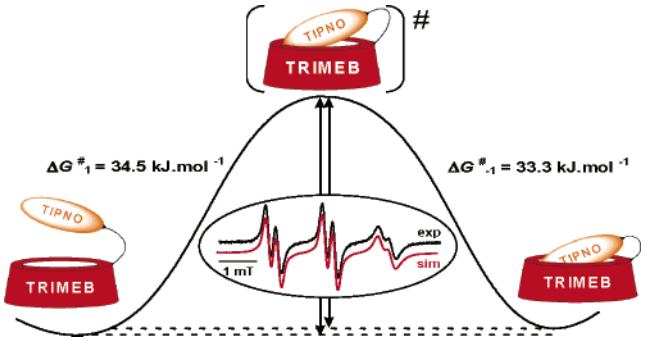

236CDTIPNO, a derivative of the persistent free radical TIPNO (1,1-dimethylethyl 2-methyl-1-phenylpropyl nitroxide) covalently bound to a permethylated-β-cyclodextrin, was prepared. Self-association of 236CDTIPNO in water was proved by solvent- and competition-dependent EPR spectroscopy experiments with 2,6-di-*O*-Me-β-cyclodextrin (DIMEB) and permethylated-β-cyclodextrin (TRIMEB) as external hosts competing for accommodation of the TIPNO moiety. Temperature-dependent EPR spectra were simulated with a novel two-dimensional (field-temperature) EPR simulation program that afforded a full determination of the thermodynamic parameters characterizing the rate constants of the self-inclusion reaction derived from Arrhenius and Eyring models. This method allows separating the line broadening effects due to relaxation from a chemical exchange, even if only the fast exchange regime is accessible experimentally. The activation parameters for the forward and backward steps were consistent with an equilibrium between a nonassociated form and a weakly associated form, with activation free enthalpies for each reaction of around 34 kJ·mol^{-1}.

Introduction

To enhance the superoxide radical detection, cyclodextrins (CDs) are interesting supramolecular assistants for EPR spin trapping experiments involving linear[1,2] or cyclic[3] nitrones. The affinity of nitrone spin traps for CDs is substantial in most cases,[2,4] but CDs exhibit higher binding constants for the corresponding superoxide spin adducts ($K_{NO\bullet} > K_{N+O-}$).[2] The binding modes of these nitroxides with CDs depend on the homotopic or heterotopic nature of the spin adducts.[2,5,6] Recently, we have reported that CDs play an important role in stabilizing the superoxide spin adduct, leading to EPR signal enhancement and in increasing the partial resistance of the nitroxide against biomimetic reductive conditions.[1−3]

However, the need for high CD concentrations can constitute an important drawback for in vivo EPR spin trapping or for therapeutic applications. Moreover, once the complex is dis-

* To whom correspondence should be addressed. Tel: + 33 491 288 927. Fax: + 33 491 288 758.
[†] Aix-Marseille Université.
[‡] Institute of Structural Chemistry.
[§] Cyclolab Ltd.

(1) Karoui, H.; Tordo, P. *Tetrahedron Lett.* **2004**, *45*, 1043−1045.
(2) Bardelang, D.; Rockenbauer, A.; Finet, J.-P.; Karoui, H.; Tordo, P. *J. Phys. Chem. B* **2005**, *109*, 10521−10530.
(3) Karoui, H.; Rockenbauer, A.; Pietri, S.; Tordo, P. *Chem. Commun.* **2002**, *24*, 3030−3031.
(4) Bardelang, D.; Clement, J.-L.; Finet, J.-P.; Karoui, H.; Tordo, P. *J. Phys. Chem. B* **2004**, *108*, 8054−8061.
(5) Lehn, J.-M. *Supramolecular Chemistry*; VCH: Weinheim, Germany, 1995.
(6) Steed, J. W.; Atwood, J. L. *Supramolecular Chemistry*; J. Wiley & Sons: Chichester, UK, 2000.

10.1021/jo061194p CCC: $33.50
Published on Web 09/02/2006

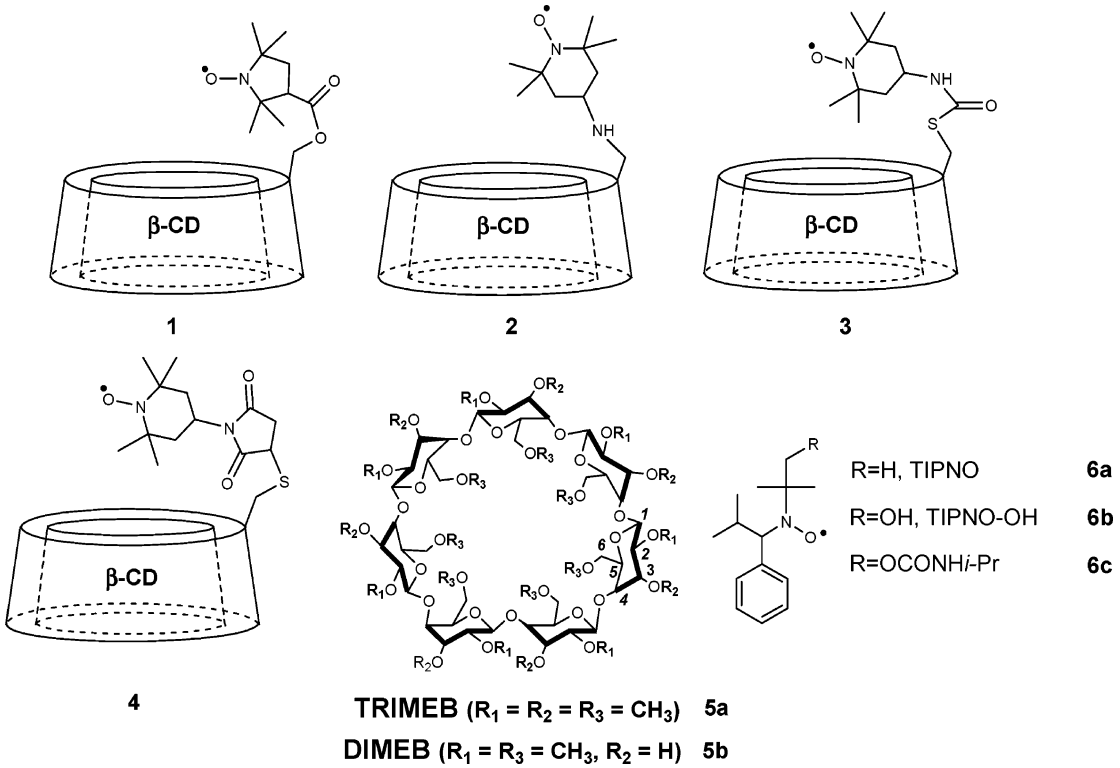

FIGURE 1. Chemical structures of the nitroxide-containing β-CDs **1**, **2**, **3**, and **4**, permethylated-β-cyclodextrin (TRIMEB) **5a**, 2,6-di-*O*-Me-β-cyclodextrin (DIMEB) **5b**, and nitroxide derivatives **6a**, **6b**, and **6c**.

solved in a biological milieu, the difference of affinity of the respective partners toward the various compartments, lipophilic or hydrophilic, can result in separation of the guest from the host. These limitations encouraged us to investigate the spin trapping behavior of functionalized nitrone spin traps covalently bound to a cyclodextrin toward self-recognition. Control of the spin adduct stabilization could be achieved at lower CD concentration, by designing a nitrone, in which the balance between the affinities of the two species for CD (nitrone before and nitroxide after spin trapping) would be shifted in favor of the nitroxide.

Before addressing the study of such compounds, the synthesis of a persistent nitroxide covalently attached to a β-cyclodextrin was necessary to verify the self-inclusion of this type of spin-labeled products in water. Cyclic and linear nitroxides have been used to investigate supramolecular entities[7] via simple or multiple association toward macropolycycles (cyclophane[8] and especially cyclodextrins[9−12]), but few examples deal with nitroxides attached to cavity-containing molecules. Rebek and co-workers[13] have reported the molecular recognition of small molecules by a resorcinarene bearing four TEMPO units. The first covalent proxyl-type nitroxide bound to a cyclodextrin **1** was described in 1970, but the properties of the host−guest complexation were not investigated (Figure 1).[14] Recently, Ionita and Chechik reported the preparation of three TEMPO derivatives appended to natural β-cyclodextrins **2**, **3**, and **4** as hosts for large supramolecular assemblies (Figure 1).[15]

We now report the synthesis of 236CDTIPNO **14**, a permethylated-β-cyclodextrin **5a** linked to a derivative of the persistent free radical TIPNO (1,1-dimethylethyl 2-methyl-1-phenylpropyl nitroxide),[16] **6a** (Figure 1), which corresponds to the spin adduct of the 2-propyl radical with PBN (2-phenyl-*N*-*tert*-butylnitrone). The nitroxide−cyclodextrin proximity is of particular importance since the respective molecular diffusions for both host and guest are no longer a limitation for the complexation process, provided the spacer is flexible enough to avoid interfering with the self-inclusion phenomenon. The choice of the permethylated-β-cyclodextrin as cyclodextrin platform was motivated by (i) the limitation of competing reactions by permethylation of the hydroxy groups, and (ii) the weak interaction between a nitrone and the host, required in spin trapping applications. However, permethylation of the hydroxy groups of each glucopyranose ring is responsible for the loss of the intramolecular hydrogen bonding network on the secondary rim, leading to a less organized and more flexible structure of the host. A carbamate function was selected as the spacer between the nitroxide and the host walls because of the

(7) Franchi, P.; Lucarini, M.; Mezzina, E.; Pedulli, G. F. *Curr. Org. Chem.* **2004**, *8*, 1831−1849 and references therein.
(8) Janzen, E. G.; Kotake, Y.; Diederich, F. N.; Sanford, E. M. *J. Org. Chem.* **1989**, *54*, 5421−5422.
(9) Franchi, P.; Lucarini, M.; Mezzina, E.; Pedulli, G. F. *J. Am. Chem. Soc.* **2004**, *126*, 4343−4354.
(10) Lucarini, M.; Luppi, B.; Pedulli, G. F.; Roberts, B. P. *Chem.−Eur. J.* **1999**, *5*, 2048−2054 and references therein.
(11) Kotake, Y.; Janzen, E. G. *J. Am. Chem. Soc*. **1992**, *114*, 2872−2874 and references therein.
(12) Martinie, J.; Michon, J.; Rassat, A. *J. Am. Chem. Soc*. **1975**, *97*, 1818−1823.
(13) Kröck, L.; Shivanyuk, A.; Goodin, D. B.; Rebek, J. J. *Chem. Commun.* **2004**, 272−273.
(14) Paton, R. M.; Kaiser, E. T. *J. Am. Chem. Soc.* **1970**, *92*, 4723−4725.
(15) Ionita, G.; Chechik, V. *Org. Biomol. Chem.* **2005**, *3*, 3096−3098.
(16) (a) Maillard, P.; Massot, J. C.; Giannotti, C. *J. Organomet. Chem.* **1978**, *159*, 219−227. (b) Grimaldi, S.; Finet, J.-P.; Zeghdaoui, A.; Tordo, P.; Benoit, D.; Gnanou, Y.; Fontanille, M.; Nicol, P.; Pierson, J.-F. *Polym. Prepr.* **1997**, *38*, 651−652. (c) Benoit, D.; Chaplinski, V.; Braslau, R.; Hawker, C. J. *J. Am. Chem. Soc.* **1999**, *121*, 3904−3920.

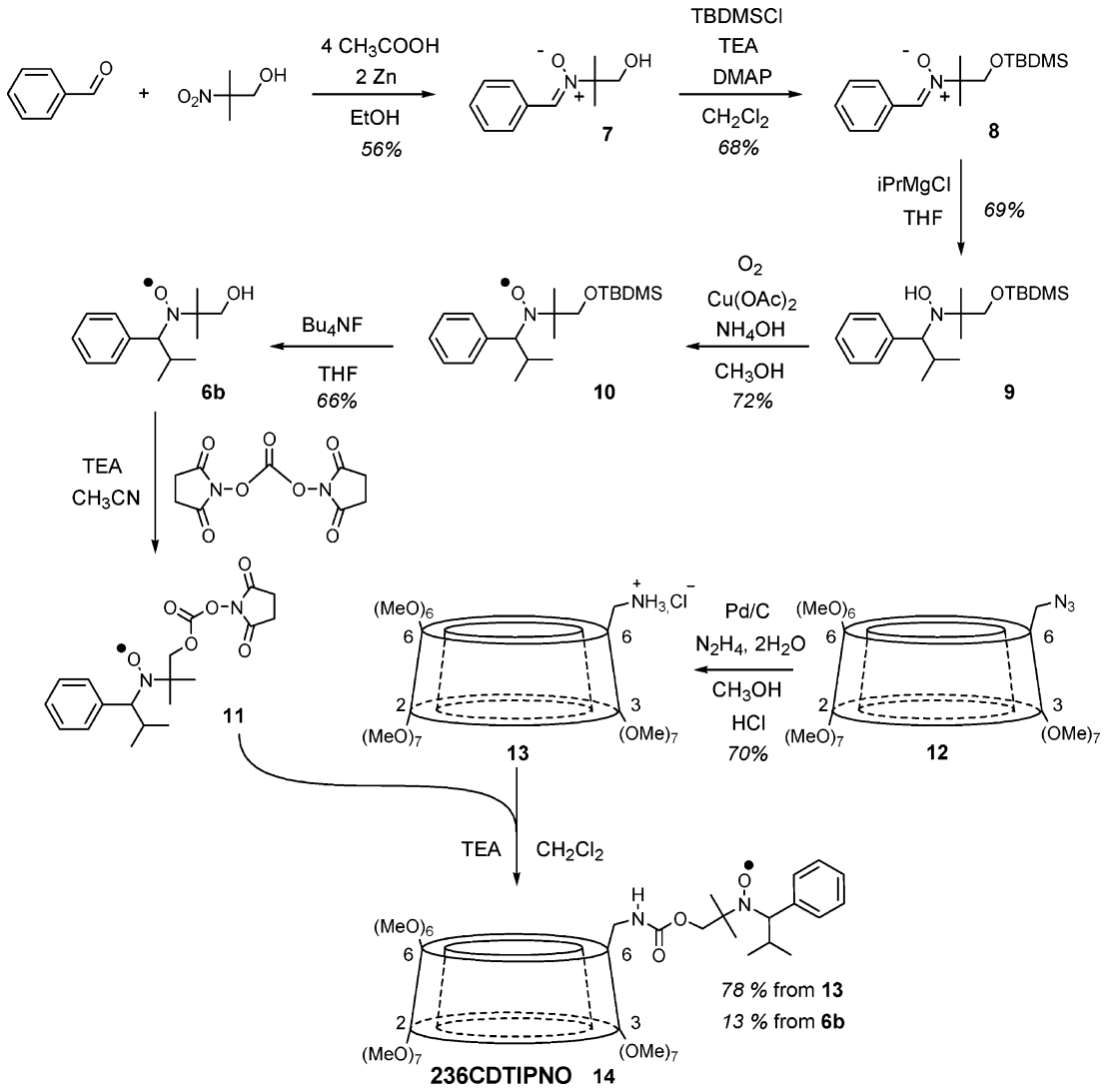

FIGURE 2. Synthesis of **14**, a TIPNO nitroxide linked to a permethylated-β-CD.

incompatibility of other systems (for example, thioether that can interfere with spin trapping)[17] in foreseeing extension of the sequence to the synthesis of nitrone−CD-type spin traps. Investigation of the binding modes of this paramagnetic species and temperature-dependent EPR spectroscopy studies gave thermodynamic and kinetic insights of the nitroxide self-inclusion reaction for the first time. The activation parameters of self-inclusion reactions have been extensively investigated for bimolecular inclusion systems involving cyclodextrins[18−21] but scarcely with a nitroxide as guest.[22]

Results and Discussion

Synthesis of 236CDTIPNO, a Covalent TIPNO-Permethylated-β-CD Derivative. A cyclodextrin derivative covalently bound to a persistent TIPNO-derived nitroxide was prepared (Figure 2). The lack of discrimination between the two rims of the β-CD cavity in the complexation of PBN[4] encouraged us to graft the TIPNO moiety on the more easily accessible C-6 position of the primary rim. Furthermore, the preferential recognition of the phenyl moiety in the PBN case[4] suggested grafting the nitroxide by the *tert*-butyl group. Thus, compound **6b**, a hydroxyl derivative of TIPNO, was prepared in five steps by the method of Klaerner and co-workers.[23] Reaction of **6b** with disuccinimidocarbonate in the presence of triethylamine afforded the crude TIPNO carbonate **11** that was directly treated with 6-monoamino-6-monodeoxy-*O*-permethyl-β-cyclodextrin[24] **13** in dichloromethane in the presence of triethylamine to afford the CD−nitroxide **14** in 78% yield, based on the cyclodextrin.

(17) Durand, G.; Polidori, A.; Ouari, O.; Tordo, P.; Geromel, V.; Rustin, P.; Pucci, B. *J. Med. Chem.* **2003**, *46*, 5230−5237.

(18) Saudan, S.; Dunand, F. A.; Abou-Hamdan, A.; Bugnon, P.; Lye, P. G.; Lincoln, S. F.; Merbach, A. E. *J. Am. Chem. Soc.* **2001**, *123*, 10290−10298.

(19) Lock, J. S.; May, B. L.; Clements, P.; Lincoln, S. F.; Easton, C. J. *Org. Biomol. Chem.* **2004**, *2*, 337−344.

(20) Ghosh, M.; Zhang, R.; Lawler, R. G.; Seto, C. T. *J. Org. Chem.* **2000**, *65*, 735−741.

(21) Cramer, F.; Saenger, W.; Spatz, H.-C. *J. Am. Chem. Soc.* **1967**, *89*, 14−20.

(22) Franchi, P.; Lucarini, M.; Pedulli, G. F.; Sciotto, D. *Angew. Chem., Int. Ed.* **2000**, *39*, 263−266.

(23) Klaerner, G.; Safir, A.; Nielsen, R.; Jandeleit, B.; Huefner, P.; Li, Y. PCT Int. Appl. **2000**, WO 200053640; *Chem. Abstr.* **2000**, *133*, 646046.

(24) Jicsinszky, L.; Iványi, R. *Carbohydr. Polym.* **2001**, *45*, 139−145.

TABLE 1. EPR Parameters[a] of the 6a-TRIMEB, 6c-TRIMEB, and 6c-DIMEB Systems and Binding Constants for the Formation of 1:1 and 1:2 Complexes in Phosphate Buffer (0.1M, pH 7.4)

EPR parameters	g	a_N (mT)	a_H (mT)	α (mT)	β (mT)	γ (mT)	K (M^{-1})
				TRIMEB			
free **6a**	2.0064_5	1.63_5	0.24_9	0.02_1	0.00_2	0.00_7	
1:1 complex	2.0065_4	1.59_8	0.25_6	0.03_0	0.01_5	0.01_6	$K_1 = 54$[b]
1:2 complex	2.0067_3	1.52_8	0.26_0	0.12_8	0.05_3	0.06_4	$K_2 = 78$[c]
free **6c**	2.0064_7	1.59_5	0.26_7	0.02_5	0.00_3	0.00_6	
1:1 complex	2.0065_1	1.55_0	0.26_9	0.04_1	0.05_4	0.04_7	$K_1 = 38$[d]
1:2 complex	2.0064_8	1.52_5	0.26_2	0.14_0	0.06_6	0.08_4	$K_2 = 33$[e]
				6c-DIMEB			
1:1 complex	2.0067_4	1.52_8	0.28_7	0.04_6	0.03_0	0.03_5	$K_1 = 6745$[d]
1:2 complex	2.0066_1	1.54_4	0.28_4	0.14_9	0.08_9	0.10_6	$K_2 = 18$[e]

[a] Accuracies of the EPR parameters are on the 5th digit for the Landé factor g and 3rd digit for hyperfine coupling constants a_N and a_H, and the relaxation parameters. [b] $K_1 = [\mathbf{6a},CD]/[\mathbf{6a}] \times [CD]$ with **6a**,CD = 1:1 complex. [c] $K_{12} = [CD,\mathbf{6a},CD]/[\mathbf{6a}] \times [CD] \times [CD]$ with $K_{12} = K_2 \times K_1$ and CD,**6a**,CD = 1:2 complex. [d] $K_1 = [\mathbf{6c},CD]/[\mathbf{6c}] \times [CD]$ with **6c**,CD = 1:1 complex. [e] $K_{12} = [CD,\mathbf{6c},CD]/[\mathbf{6c}] \times [CD] \times [CD]$, with $K_{12} = K_2 \times K_1$ and CD,**6c**,CD = 1:2 complex.

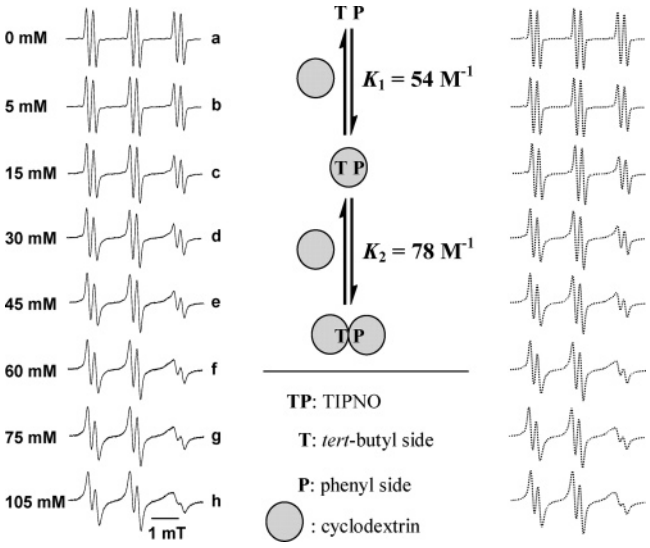

FIGURE 3. EPR titration of **6a** in the presence of **5a** in phosphate buffer: (left column) (—) experimental spectra, (right column) (···) simulated spectra.

Moreover, a second related TIPNO carbamate derivative **6c** was prepared to evaluate the possible influence of the linker group on the EPR spectrum, which could interfere with the effect of the CD complexation. Carbamate **6c** was obtained by condensation of the TIPNO carbonate **11** with isopropylamine in the presence of triethylamine.

EPR Study of the Noncovalent Interactions in Complexes 6a/TRIMEB, 6c/TRIMEB, and 6c/DIMEB. To study the interactions between nitroxides **6a** or **6c** and cyclodextrin derivatives, EPR titrations of the nitroxides **6a** or **6c** in the presence of TRIMEB **5a** and DIMEB **5b** were performed with increasing concentrations of the cyclodextrin derivative in an aqueous stock solution of TIPNO (Table 1 and Figure 3). To decompose the EPR spectra recorded with the different cyclodextrin concentrations (Figure 3), the two-dimensional field concentration simulation program was utilized.[25] This method allows obtaining a unique decomposition even in the case when individual spectra do not have adequate amounts of information to determine the EPR parameters for the species formed in the course of association. In the simulation, the parameters are simultaneously optimized for both the mass balance equation (the two binding constants K_1 and K_2) and the EPR spectra (g-factors, hyperfine coupling constants, relaxation parameters). Since the lines of the nonassociated and associated components were not resolved, we could not decide a priori whether the rate of association was slow or fast on the EPR time scale. For this reason, the spectra were computed either as a superimposition of the components, corresponding to the case of a slow association, or by using the weight-averaged parameters (g-factors, hyperfine coupling constants, relaxation parameters), corresponding to the case of a fast association. Both assumptions gave nearly the same K_1 and K_2 binding constants (see Figure 3), and the quality of fit was also similar, thus the data were not adequate to decide whether the rate of association is slow or fast. The EPR parameters obtained by the slow association model are reported in Table 1. Titrations of the TIPNO carbamate derivative **6c** in the presence of **5a** or **5b** were also performed under similar experimental conditions (Table 1).

Excellent simulations in the whole domain of CD concentrations (see Supporting Information) could only be achieved by assuming a single (1:1 complex, K_1) and a double (1:2 complex, K_2) association, typical of a stepwise binding process (Table 1 and Figure 3). The absence of a second type of 1:1 complexes has already been reported by Lucarini and co-workers[9] for chiral heteroditopic nitroxide−DIMEB complexes and attributed to a conformational preference of the CD. Interestingly, Lucarini and co-workers[9] noted the absence of formation of a complex between their chiral nitroxides and TRIMEB, their nitroxides being a priori less bulky than **6a** and **6c**. In the case of **6a** and **6c**, significant changes are only observed for CD concentrations higher than 15 mM (Figure 3).

Both **6a** and **6c** exhibit similar values of K_1 (54 and 38, respectively) for formation of the 1:1 complexes with TRIMEB, likely due to inclusion of the same aromatic fragment in the cyclodextrin cavity.[26] This is in good agreement with the close values of $\Delta a_N = a_{N,free} - a_{N,in}$ (0.037 mT for **6a** and 0.045 mT for **6c**). The decrease of a_N agrees with the less polar lattice of the nitroxide moiety expected after inclusion in the CD cavity. However, as noted by Lucarini and co-workers,[9] changes of $a_{H\beta}$, which is sensitive to both the spin density on the nitrogen atom and the dihedral angle $<H_\beta-C-N-2p_z>$, would be expected. In fact, the absence of significant changes (Table 1) can be due to a compensation effect between the decrease of spin density on the nitrogen atom ($\Delta a_N > 0$) and conformational changes linked to the inclusion (increase of $<H_\beta-C-N-2p_z>$ angle).

The interactions between nitroxides **6a** and **6c** and **5a** (Table 1) are weak, and the formation of 1:2 complexes requires very high CD concentrations (Figure 3). For **6a**, the formation of the 1:2 complex is slightly cooperative ($K_2 > K_1$). In the case of **6c**, no cooperativity takes place ($K_2 > K_1$) due to an energetic cost, resulting from either desolvation of the polar amide moiety or from the lesser hydrophobicity of the CH_2OCONH*i*-Pr group. In the second step, the better complexation of the *t*-Bu fragment in **6a** is emphasized by the larger value of $\Delta' a_N = a_{N,1:1} -$

(25) Rockenbauer, A.; Szabó-Plánka, T.; Árkosi, Sz.; Korecz, L. *J. Am. Chem. Soc.* **2001**, *123*, 7646−7654.

(26) The 1:1 complex with the *t*-Bu group included in the cyclodextrin was disregarded because very low (more than 1 order less) binding constant was obtained.

TABLE 2. EPR Parameters[a] of Nitroxides 6a, 6b, 6c, and 14 in Various Solvents

nitroxide	species (%)	solvent	g	a_N (mT)	a_H (mT)	α (mT)	β (mT)
6a	100	water[b]	2.0064_5	1.63_5	0.24_9	0.02_1	0.00_2
6b	100	water[b]	2.0064_7	1.59_8	0.26_3	0.02_4	0.00_3
6c	100	water[b]	2.0064_7	1.59_5	0.26_7	0.02_5	0.00_3
6c	100	*t*-BuPh	2.0069_1	1.44_6	0.28_6	0.03_1	0.01_1
14	100[c]	$CDCl_3$	2.0069_0	1.47_2	0.26_4	0.10_9	0.01_3
14	100[c]	toluene	2.0069_7	1.44_1	0.26_7	0.07_4	0.00_1
14	100[c]	*t*-BuPh	2.0069_9	1.43_7	0.27_0	0.08_0	0.01_8
14	38 (A)[c]	water[b]	2.0067_5	1.54_3	0.26_4	0.04_3	0.03_5
	62 (B)[d]		2.0064_6	1.57_1	0.25_2	0.25_0	0.02_1

[a] Accuracies of the EPR parameters are on the 5th digit for the Landé factor g and 3rd digit for hyperfine coupling constants a_N and a_H, and the relaxation parameters. [b] Chelex-treated aqueous phosphate buffer (0.1 M, pH 7.4). [c] Weakly included species. [d] Nonincluded species.

$a_{N,1:2}$ for formation of the 1:2 complex for **6a** ($\Delta' a_N = 0.070$ mT) than for **6c** ($\Delta' a_N = 0.025$ mT). As expected for inclusion of a nonchiral fragment, the $a_{H\beta}$ values do not change significantly (variations of 0.004 and −0.007 mT for **6a** and **6c**, respectively).

It is worthwhile noting that K_1 for the formation of the **6c**−DIMEB 1:1 complex is more than 150 times greater than K_1 for formation of the **6c**−TRIMEB 1:1 complex. This is likely due to an easier access to the DIMEB cavity (with a non-methylated hydroxyl group in the position 3) for **6c**. In their nitroxide−DIMEB systems, Lucarini and co-workers[9] observed smaller K values probably because their nitroxides are less hydrophobic than **6c** (*i*-Pr and phenyl groups). More surprising is the increase of a_N ($\Delta' a_N = -0.016$ mT) for the formation of the 1:2 complex of **6c** with DIMEB. It has already been reported[27] that the intramolecular hydrogen bond (IHB) matched the polar effect of electron-withdrawing groups with an increase of the a_N value with increasing IHB strength. The presence of one free hydroxyl group on each pyranose unit leads the CD cavity to exhibit different shapes for DIMEB and for TRIMEB. Hence, the DIMEB cavity can accommodate **6c** in a way favoring either an intermolecular hydrogen bond between the nitroxide moiety of **6c** and one or several of the free hydroxyl groups carried by the CD cavity, or an intramolecular hydrogen bond with the H atom of the amide function. The comments on $a_{H\beta}$ done for the formation of the complexes involving TRIMEB and **6a** or **6c** hold for the DIMEB−**6c** system.

The significant increase of the relaxation parameters α, β, and γ in each system (Table 1) denotes that the association with CD slows down the rotational motion of the nitroxide. It is worth noting that the relaxation parameters α, β, and γ for the 1:1 and 1:2 **6c**−TRIMEB complexes are slightly greater than those for the homologous **6a**−TRIMEB complexes. This can be related to the difference of steric bulkiness between CMe_2CH_2-OCONH*i*-Pr and the *t*-Bu group. On the other hand, 1:1 and 1:2 complexes of **6c** with DIMEB and TRIMEB exhibit very similar relaxation parameters. Thus, despite a weak molecular recognition, these data show that TRIMEB can bind TIPNO derivatives.

EPR Study of 236CDTIPNO, 14. When the EPR spectra of the three different free nitroxides **6a**, **6b**, and **6c** in aqueous solutions are compared, a clear decrease[27] of a_N (Table 2) is observed, and it can be correlated with the electron-withdrawing capacity of the substituent:[28] Me ($\sigma_I = -0.01$) to CH_2OH ($\sigma_I = 0.11$)[27] and CH_2OCONH*i*-Pr ($\sigma_I = 0.17$). The a_N values of **6a**, **6b**, and **6c** are greater in water than in organic solvents because

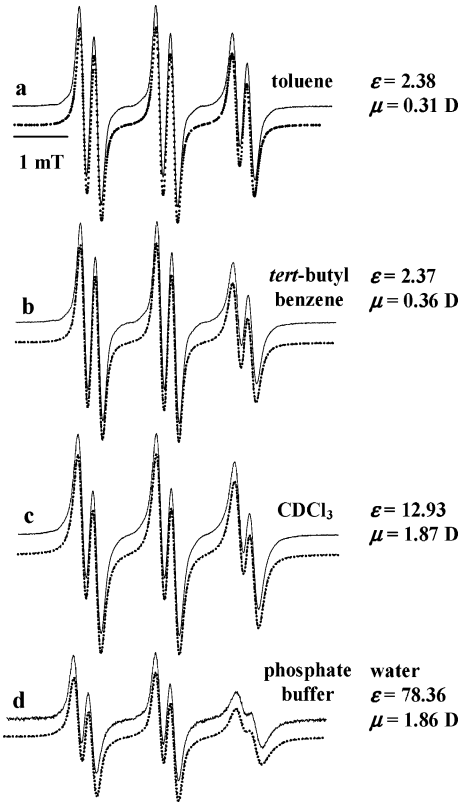

FIGURE 4. EPR spectra of 236CDTIPNO **14** (5×10^{-4} M) in organic and aqueous media: (upper curve) (—) experimental spectra, (lower curve) (···) simulated spectra.

of the stabilization of the charged canonic form of the nitroxide moiety in water.[29] The slight changes of $a_{H\beta}$ denote minor changes in the conformations. The EPR spectra of **14** recorded in $CDCl_3$, toluene, and *tert*-butylbenzene were satisfactorily simulated assuming the existence of only one species (Figure 4). The ESR parameters of **14** in *tert*-butylbenzene ($a_N = 1.437$ mT and $a_H = 0.270$ mT) are very close to those reported for **6c** ($a_N = 1.446$ mT and $a_H = 0.286$ mT), a good model for the CD-bound nitroxide **14** with a nonincluded TIPNO moiety (see Table 2). The CD-included forms could not be detected in the three organic solvents. When going from *tert*-butylbenzene, toluene to $CDCl_3$, the a_N value increases with the solvent polarity. [29,30] It is noteworthy that the relaxation parameters α and β are nearly insensitive to the polarity of the organic solvents. The observed reduction of the tumbling rate is characteristic of nitroxides attached to bulky molecules.[31] Moreover, whatever the solvent, comparison of the EPR spectra of **6c** and **14** reveals an increase of the relaxation parameters α and β with the increasing size of the molecule (Table 2). The relaxation parameter γ followed an identical trend as parameter β.

In aqueous solution, the asymmetry of the EPR spectrum of **14** is more pronounced with stronger line broadening, particu-

(27) Marque, S.; Fischer, H.; Baier, E.; Studer, A. *J. Org. Chem.* **2001**, *66*, 1146−1156.
(28) Charton, M. *Prog. Phys. Org. Chem.* **1981**, *13*, 119−251.
(29) Beckwith, A. L. J.; Bowry, V. W.; Ingold, K. U. *J. Am. Chem. Soc.* **1992**, *114*, 4983−4992.
(30) Herrenschmidt, Y.-L.; Guetté, J.-P. Constantes Physico-chimiques. In *Techniques de l'Ingénieur*; Editions T. I.: Paris, France, 1988; pp K310−311.
(31) Clément, J.-L.; Gilbert, B. C.; Rockenbauer, A.; Tordo, P. *J. Chem. Soc., Perkin Trans. 2* **2001**, 1463−1470.

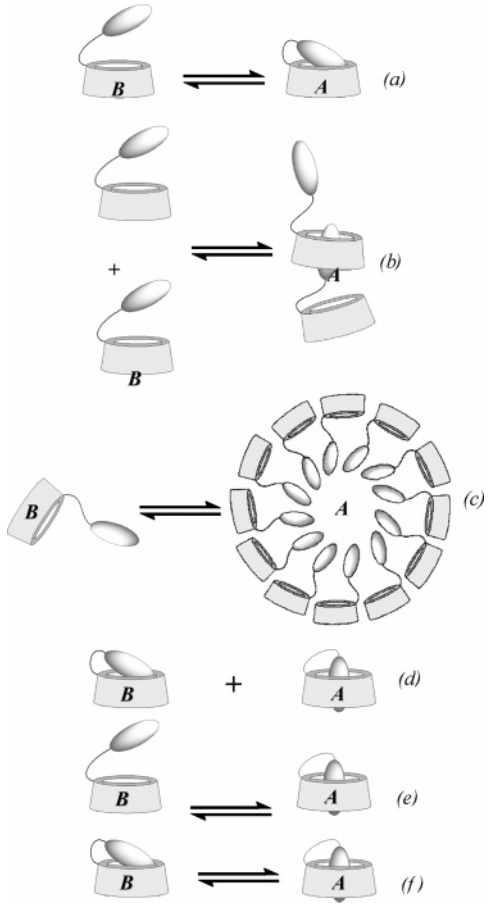

FIGURE 5. Possible modes of binding of 236CDTIPNO **14** in water.

larly, for the two lines at high magnetic field (Figure 4, spectrum d). In this case, a good simulation could be achieved only by assuming the existence of two nearly equally populated species that are undergoing a fast exchange (Table 2).

Cyclodextrins are considered as polar molecules with a nonpolar cavity. Hence, when a nitroxide is attached to CD, a slight decrease (0.01−0.02) of a_N due to the presence of a fairly electron-withdrawing group (cyclodextrin contains 35 oxygen atoms out of 210 atoms) can be expected. Thus, the small Δa_N (0.024 mT) between **6c** and **14B** led us to consider species **B** as exhibiting the nitroxide moiety outside of the inner cavity. The small Δa_N (0.028 mT) between species **A** and **B** (Table 2) does not agree with a strongly included nitroxide moiety—1:2 complex ($\Delta a_N = 0.070$ mT and a_N expected smaller than 1.525 mT) or 1:1 complex ($\Delta a_N = 0.045$ mT)—for species **A**. Thus, species **A** is likely to be a weakly associated nitroxide, with the nitroxide moiety located amidst the methoxy crown of the narrow rim of the CD cavity, as depicted in Figure 5a. However, several alternative possibilities, displayed in Figure 5b−f, cannot be excluded. The concentration independence of the EPR spectrum of **14** in the 10^{-5} to 10^{-3} M range is in favor of a reversible intramolecular model[32−40] (Figure 5a,d−f) rather than an intermolecular one[41,42] (Figure 5b). The formation of micellar-type structures, such as that depicted in Figure 5c, with the hydrophobic TIPNO part self-organized keeping the hydrophilic cyclodextrin moiety on the outer sphere of the micelle could be considered.[43−45] However, the spin−spin interactions between the nitroxide functions of the 236CDTIPNO molecules that are expected in a micellar model even at low nitroxide concentrations were not observed. Only at concentrations higher than 5×10^{-3} M further line broadening was observed that can be attributed to the spin−spin interactions classically occurring at high concentrations of nitroxides.[46,47] Addition of dioxane, known to disorganize micelles, to the nitroxide solution (up to 40% v/v) failed to modify the EPR spectrum.[48] Furthermore, a broader line width is expected for the higher level of organization corresponding to a micelle architecture, but the observed values of the line width of the two species, $\Delta H_{pp}^{\mathbf{A}} = 0.046$ mT (weakly associated) and $\Delta H_{pp}^{\mathbf{B}} = 0.250$ mT (nonassociated), follow an opposite trend, thus excluding the micellar model (Figure 5c). The alternative possibility involving the presence of two diastereoisomers with different association constants, resulting from enantiomeric discrimination between the two enantiomers of the TIPNO moiety by the chiral cyclodextrin (Figure 5d)—known for amino acid functionalized β-CD—was disregarded (see Experimental Section).[49−52] Equilibria between nonassociated and strongly associated species (Figure 5e) or between weakly associated and strongly associated species (Figure 5f) are also possible. These two possibilities are discarded due to the a_N values observed (vide supra) which are noncompatible.

The α relaxation parameter, smaller for species **A** (0.043 mT) than for species **B** (0.250 mT), means that the weakly self-associated species exhibits a more compact geometry, allowing a faster rotation. Indeed, if the molecule is not self-associated,

(32) Liu, Y.; Zhao, Y.-L.; Zhang, H.-Y.; Fan, Z.; Wen, G.-D.; Ding, F. *J. Phys. Chem. B* **2004**, *108*, 8836−8843.
(33) Liu, Y.; You, C.-C.; Zhang, H.-Y.; Zhao, Y. L. *Eur. J. Org. Chem.* **2003**, 1415−1422.
(34) Hamasaki, K.; Usui, S.; Ikeda, H.; Ikeda, T.; Ueno, A. *Supramol. Chem.* **1997**, *8*, 125−135.
(35) McAlpine, S. R.; Garcia-Garibay, M. A. *J. Am. Chem. Soc.* **1996**, *118*, 2750−2751.
(36) Dunbar, R. A.; Bright, F. V. *Supramol. Chem.* **1993**, *3*, 93−99.
(37) Eddaoudi, M.; Parrot-Lopez, H.; Frizon de Lamotte, S.; Ficheux, D.; Prognon, P.; Coleman, A. W. *J. Chem. Soc., Perkin Trans. 2* **1996**, 1711−1715.
(38) Bellanger, N.; Perly, B. *J. Mol. Struct.* **1992**, *273*, 215−226.
(39) Ikeda, T.; Yoshida, K.; Schneider, H.-J. *J. Am. Chem. Soc.* **1995**, *117*, 1453−1454.
(40) McAlpine, S. R.; Garcia-Garibay, M. A. *J. Org. Chem.* **1996**, *61*, 8307−8309.
(41) McAlpine, S. R.; Garcia-Garibay, M. A. *J. Am. Chem. Soc.* **1998**, *120*, 4269−4275.
(42) Liu, Y.; Fan, Z.; Zhang, H.-Y.; Yang, Y.-W.; Ding, F.; Liu, S.-X.; Wu, X.; Wada, T.; Inoue, Y. *J. Org. Chem.* **2003**, *68*, 8345−8352.
(43) Auzely-velty, R.; Pean, C.; Djedaïni-Pilard, F.; Zemb, T.; Perly, B. *Langmuir* **2001**, *17*, 504−510.
(44) Auzely-velty, R.; Djedaïni-Pilard, F.; Desert, S.; Perly, B.; Zemb, T. *Langmuir* **2000**, *16*, 3727−3734.
(45) Zhang, P.; Parrot-Lopez, H.; Tchoreloff, P.; Baszkin, A.; Ling, C. C.; De Rango, C.; Coleman, A. W. *J. Phys. Org. Chem.* **1992**, *5*, 518−528.
(46) Bratt, P. J.; Kevan, L. *J. Phys. Chem.* **1993**, *97*, 7371−7374.
(47) Gerson, F.; Huber, W. *Electron Spin Resonance Spectroscopy of Organic Radicals*; Wiley-VCH: Heppenheim, Germany, 2003.
(48) Chalier, F.; Ouari, O.; Tordo, P. *Org. Biomol. Chem.* **2004**, *2*, 927−934.
(49) Parrot-Lopez, H.; Galons, H.; Coleman, A. W.; Djedaïni, F.; Keller, N.; Perly, B. *Tetrahedron: Asymmetry* **1990**, *1*, 367−370.
(50) Wang, H.; Cao, R.; Ke, C.-F.; Liu, Y.; Wada, T.; Inoue, Y. *J. Org. Chem.* **2005**, *70*, 8703−8711.
(51) Ikeda, H.; Nakamura, M.; Ise, N.; Oguma, N.; Nakamura, A.; Ikeda, T.; Toda, F.; Ueno, A. *J. Am. Chem. Soc.* **1996**, *118*, 10980−10988.
(52) One referee suggested that the spectra recorded might be described by a fast exchange between weakly included species—one diastereoisomer and a mixture of both diastereoisomers not included in the cavity, i.e., a combination of enantioselection and fast exchange; Figure 5a and d. This possibility cannot be ruled out with the available data. However, this complex scheme was not taken into account.

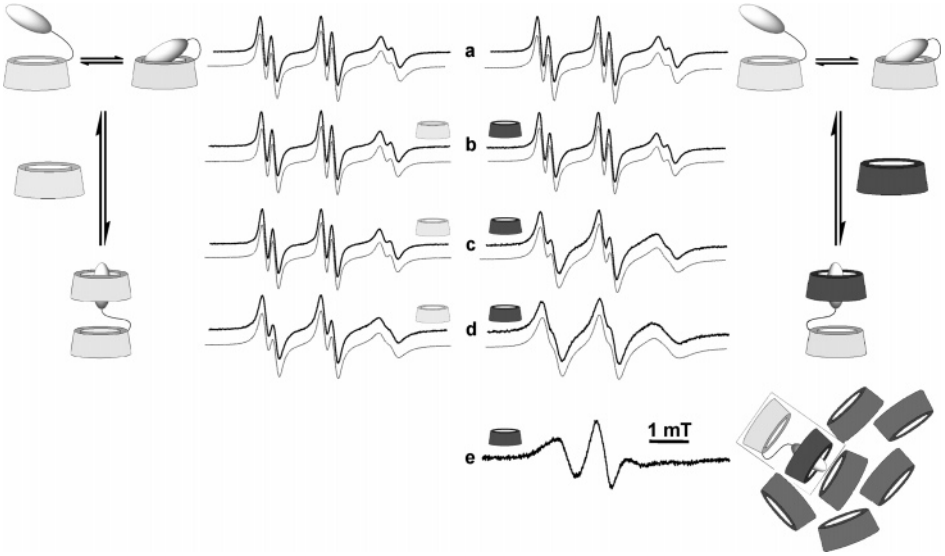

FIGURE 6. Competition experiments between 236CDTIPNO **14** and cyclodextrins as external competing hosts: (a) **14** (5×10^{-4} M) alone and with a CD (b) 1 equiv, (c) 10 equiv, (d) 100 equiv, (e) 300 equiv. Left column: TRIMEB (light gray annulus). Right column: DIMEB (dark gray annulus): (upper curve) (—) experiments, (lower curve) (···) simulations.

TABLE 3. EPR Parameters[a] of A and B Species in Fast Exchange, Representative of the Two Conformers of 14[b] in the Absence and Presence of β-CD Derivatives as Competing Hosts

			a_N (mT)		Populations (%)		α (mT)		β (mT)	
entry	CD	equiv	**A**	**B**	**A**	**B**	**A**	**B**	**A**	**B**
1	no	0	1.54_3	1.57_1	52	48	0.04_3	0.25_0	0.03_5	0.02_1
2	DIMEB	1	1.54_2	1.54_0	45	55	0.04_9	0.20_1	0.03_6	0.06_4
3		10	1.52_2	1.48_7	22	78	0.06_8	0.20_6	0.05_2	0.09_9
4		100	1.44_6	1.49_4	8	92	0.07_8	0.22_3	0.05_3	0.12_4
5	TRIMEB	1	1.54_3	1.56_9	57	43	0.04_9	0.19_6	0.03_4	0.02_7
6		10	1.54_2	1.57_1	53	47	0.04_9	0.20_4	0.03_6	0.03_6
7		100	1.52_6	1.55_1	28	72	0.05_8	0.21_1	0.05_0	0.08_9

[a] Accuracies of the EPR parameters are on the 5th digit for the Landé factor *g* and 3rd digit for hyperfine coupling constants a_N and a_H, and the relaxation parameters. [b] 5×10^{-4} M.

the moment of inertia will be rather large, due to the long linear size of the molecule. If the effective radius is reduced by self-association, the rotation will be accelerated, resulting in a narrower line width.[53]

To get better insight in the species involved in the host–guest equilibrium, addition of TRIMEB or DIMEB as external competing complexation hosts was performed and showed important changes in the pattern of the EPR spectra of **14** (Figure 6).

An increasing anisotropy of the EPR spectrum of **14** is observed with increasing concentrations of the competing cyclodextrins, and that is likely due to a progressive nitroxide immobilization by bimolecular encapsulation of the TIPNO moiety. The difference in binding behavior of the two competing methylated CDs is revealed by the similar variations of the EPR spectrum, detected on the **B** form of **14** (Table 3, entries 3 and 7). This effect is underlined by the same a_N values for species **A** with 10 equiv of DIMEB and 100 equiv of TRIMEB. EPR spectra were correctly simulated assuming two species **A** and **B** (Table 3, Figure 7), even though more species are present. Thus, the spectrum of species **B** is an average of the spectra of the nonincluded species γ and the intermolecular included species δ, whereas the spectrum of the species **A** is an average

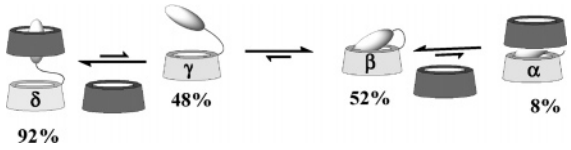

FIGURE 7. Proposed binding modes for **14** in water, alone (γ and β), or in the presence (δ, γ, β, and α) of DIMEB (dark gray annulus) as an external competing host.

spectrum of the weakly included species β and the weakly 1:2 complex α (Figure 7).

The higher solubility of DIMEB in water allowed the EPR spectrum of **14** to be recorded in the presence of up to 300 equiv of DIMEB. The strong asymmetry of the resulting spectrum (Figure 6e) is probably related to a marked immobilization of the nitroxide in the cavity of CD aggregates.[54] However, the pronounced anisotropy in this limiting case is close to the situation encountered in the solid state or in the folding of spin-labeled proteins.[55] Whatever the nature of the competing CD, the a_N value of the TIPNO derivative decreases with

(53) Suzuki, M.; Szejtli, J.; Szente, L. *Carbohydr. Res.* **1989**, *192*, 61–68.

(54) Loftsson, T.; Másson, M. *Proceedings of 12th International Cyclodextrin Symposium*; Montpellier, May 16–19, 2004, APGI: Chatenay-Malabry, France, pp 409–416.

(55) Holtzman, J. L. *Spin Labeling in Pharmacology*; Academic Press: Orlando, 1984.

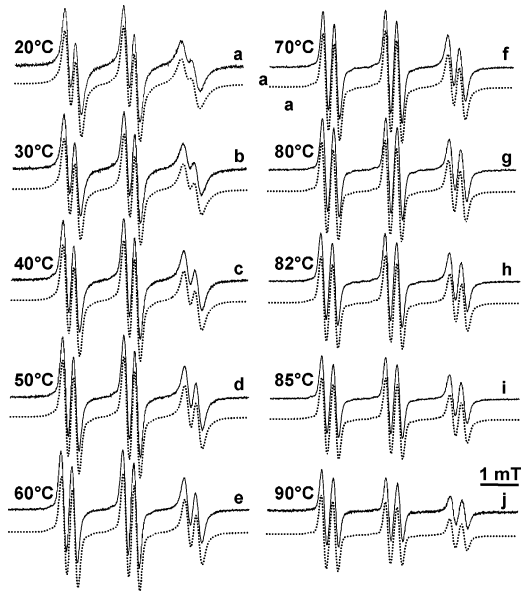

FIGURE 8. Temperature dependence of the EPR spectrum of **14** (5×10^{-4} M) in phosphate buffer solution: (upper curve) (—) experimental spectra, (lower curve) (···) simulated spectra.

increasing concentrations of the added cyclodextrins as observed for the noncovalent system. The trend is more pronounced for DIMEB when 100 equiv is added with a decrease of 0.077 mT for species **B**. Moreover, the proportion of species **B** increases from 48 to 92%. These observations can be tentatively explained by an increasing intermolecular type complexation of **14** with species **B** going from a nonincluded form to a strongly associated 1:2 complex δ (Figure 7).

A similar trend is observed for species **A**. The increase of the α and β parameters indicates once again that the molecular rotation of the nitroxide is slowed upon addition of DIMEB. In the case of the weakly self-included species β, the presence of DIMEB leads to complexation of the alkyl parts out of the methoxy crown of the narrow rim of the CD cavity to form 1:2 heterocomplexed covalent analogue α, although in a modest percentage (8%). Thus, addition of increasing amounts of methylated β-cyclodextrins favors the intermolecular binding mode, with formation of the intermolecular dimer δ (92%). Moreover, the higher value of α^B compared to α^A related to the greater flexibility of the species δ (noncovalent intermolecular type association) compared to species α (covalent intramolecular type association) is worth noting. These data are probably due to the higher rotation possibilities offered by the more compact intramolecular dimer α compared to the more extended intermolecular dimer δ.

Kinetics and Thermodynamics of the Autocomplexation of 14. The temperature dependence of the EPR spectrum of **14** (5×10^{-4} M) in aqueous phosphate buffer shows a progressive and reversible symmetrization of the signal related to the acceleration of the inclusion and exclusion rates of the TIPNO moiety in the CD cavity. Above 85 °C, decomposition of the product started to be significant (Figure 8).

The positions of the six-line spectra of **14** are determined by the isotropic g, a_N, and a_H constants. If we assume that two species are present in a slow exchange, two different sets of parameters (g^A, $a_N{}^A$, $a_H{}^A$ and g^B, $a_N{}^B$, $a_H{}^B$) will determine the positions of the lines in the superimposed spectra. If the exchange is fast, superimposed lines should not be seen anymore. Indeed, only a six-line pattern can be seen, where the position of the lines can be determined as population weighted averages (see Experimental Section). In the case of an intermediate exchange frequency, the exchange process could produce an extra line broadening proportional to $P_A P_B \delta\omega^2 \tau_{exc}$, where P_A and P_B are the respective populations, $\delta\omega$ is the difference of the frequency of the lines for the two conformers, and τ_{exc} is the average exchange time ($1/\tau_{exc} = P_A/\tau_A + P_B/\tau_B$). The lines of the nitrogen triplet will have a further broadening due to the orientation averaging of g and hyperfine anisotropy, which can be described by the usual relaxation formula, where M_N is the magnetic quantum number of ^{14}N nuclei

$$W(M_N) = \alpha + \beta M_N + \gamma M_N{}^2$$

However, the nonassociated and weakly associated forms of **14** experience different relaxations since the more compact molecule in the compact form can rotate more easily. Thus, six different relaxation parameters and the exchange time can describe the line broadening. Since there are only three independent line width data in the spectra, the unique parameter determination is impossible, when the spectra are simulated one by one. To overcome this shortcoming, we developed recently a new two-dimensional simulation approach, where the second coordinate is the temperature.[56] Then the aggregate information of n spectra offers altogether $3n$ data for the line width. In the simultaneous spectrum fitting, all spectroscopic parameters were not adjusted independently, except for the first few coefficients in their power expansion (eq 1):

$$f(T - T_0) = f_0 + f_1(T - T_0) + f_2(T - T_0)^2 + f_3(T - T_0)^3 \quad (1)$$

where $T_0 = 273$ K was used in the program.

Typically for the g-factors and the small a_H values, two coefficients were adjusted, while three and sometimes four coefficients were adjusted for a_N and the α, β, and γ relaxation parameters. Concerning the exchange time, it can be described either by the Arrhenius equation (eq 2)

$$k = 1/\tau_{exc} = A \exp(-E_a/RT) \quad (2)$$

or by the Eyring equation (eq 3)

$$k = 1/\tau_{exc} = (k_B T/h)\exp(\Delta S^{\ddagger}/R)\exp(-\Delta H^{\ddagger}/RT) \quad (3)$$

TABLE 4. Temperature Dependence of the Normalized Populations of the Weakly Associated Species A (P_A) and the Nonassociated Species B (P_B) of 14 and Kinetic Constants of the Exchange Process Given by the Arrhenius Model

T/°C	T/K	P_A	P_B	K	k_{-1}/s^{-1}	k_1/s^{-1}
20	293	0.380	0.620	0.613	8.3×10^6	5.1×10^6
30	303	0.388	0.612	0.634	8.9×10^6	5.7×10^6
40	313	0.396	0.604	0.656	9.5×10^6	6.3×10^6
50	323	0.403	0.597	0.675	10.1×10^6	6.8×10^6
60	333	0.410	0.590	0.695	10.7×10^6	7.5×10^6
70	343	0.416	0.584	0.712	11.3×10^6	8.1×10^6
80	353	0.422	0.578	0.730	11.9×10^6	8.7×10^6
82	355	0.423	0.577	0.733	12.0×10^6	8.8×10^6
85	358	0.425	0.575	0.739	12.2×10^6	9.0×10^6

(56) Rockenbauer, A.; Nagy, N. V.; Le Moigne, F.; Gigmes, D.; Tordo, P. *J. Phys. Chem.* A **2006**, *110*, 9542−9548.

TABLE 5. Thermodynamic and Kinetic Parameters for the Exchange between the Weakly and Nonassociated Species A and B of 14

	ΔG_R[a] (kJ·mol^{-1})	ΔH_R (kJ·mol^{-1})	ΔS_R (J·K^{-1}·mol^{-1})	E_a (kJ·mol^{-1})	A (s^{-1})	$\Delta G^{\ddagger}$[a] (kJ·mol^{-1})[a]	$\Delta H^{\ddagger}$ (kJ·mol^{-1})	$\Delta S^{\ddagger}$ (J·K^{-1}·mol^{-1})
Arrhenius[b]	1.2	2.5	4.5	6.6	9.6×10^7			
Eyring[b]	1.2	2.5	4.5			33.9	3.5	−102.2
association				7.9	12.6×10^7	34.5	4.8	−104.5
dissociation				5.4	7.3×10^7	33.3	2.3	−100.0

[a] At 298 K. [b] Exchange process. The errors for ΔG_R and ΔH_R are 0.2, for ΔS_R and E_a 1.0, for A 2.0×10^7, for $\Delta G^{\ddagger}$ and $\Delta H^{\ddagger}$ 2.0 and for $\Delta S^{\ddagger}$ 10.0.

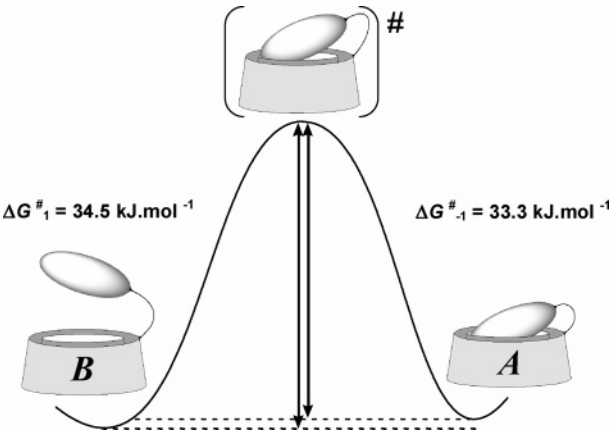

FIGURE 9. Suggested reaction pathway between the non- and the weakly associated forms of 236CDTIPNO **14** in phosphate buffer.

Furthermore, the relative populations can be given by the van't Hoff relation (eq 4):

$$K = P_A/P_B = \exp(\Delta S_R/R - \Delta H_R/RT) \quad (4)$$

Consequently, the number of adjusted parameters determining the line width could be $6 \times 3 = 18$ relaxation and 2 thermodynamic quantities in a typical two-dimensional simulation, which needs at least 7 spectra having 21 independent line width data.[57] The 2D EPR simulations give the thermodynamic quantities defined in eqs 2−4, which allow the computation of association constants K as well as the average exchange rates k. The populations of A and B can be given as $P_A = K/(1 + K)$ and $P_B = 1/(1 + K)$, respectively, while the association rate is $k_1 = kK(1 + K)/(1 + K^2)$ and the dissociation rate is $k_{-1} = k(1 + K)/(1 + K^2)$. All these data are reported in Table 4. The individual thermodynamic parameters for the association and dissociation processes were derived by eqs 5−9.

$$A_1/A_{-1} = \exp(\Delta S_R/R) \quad (5)$$

$$E_{a_1} - E_{a_{-1}} = \Delta H_R \quad (6)$$

$$\Delta G^{\ddagger}_1 - \Delta G^{\ddagger}_{-1} = \Delta G_R \quad (7)$$

$$\Delta H^{\ddagger}_1 - \Delta H^{\ddagger}_{-1} = \Delta H_R \quad (8)$$

$$\Delta S^{\ddagger}_1 - \Delta S^{\ddagger}_{-1} = \Delta S_R \quad (9)$$

In this set of experiments, populations P_A and P_B are different at 293 K in comparison with the values estimated from the rather arbitrary decomposition of a single spectrum (around 50/50). However, the confidence of the novel proportions is better as the calculations are based on a set of temperature-dependent spectra and the populations are derived from the thermodynamic relations. The data in Table 5 are only slightly affected whether we use the Arrhenius (eq 2) or the Eyring relation (eq 3) in the 2D simulations.

Statistical analyses were carried out to characterize the quality of the different models. The Eyring and Arrhenius models were compared to the cases supposing slow or fast exchanges. The respective regression coefficients R, defined in ref 25, were 0.998113, 0.998069, 0.997559, and 0.995372 in the four cases. The noise equivalent ΔR factor[25] offering the criterion for significance was 0.000024. Consequently, according to the R values, the best kinetic model was given by the Eyring equation, but the regression in the Arrhenius model was smaller only by $2\Delta R$, thus the difference cannot be considered as significant. On the other hand, the computations, assuming slow or fast exchanges, gave a significant deterioration of the fit since the drops of R were 23 and 114 times larger, respectively, than the noise equivalent ΔR change of regression. Thus, the assumption of a chemical exchange between the open and closed species is necessary to obtain a correct description for the temperature dependence of the line width in the EPR spectra of 236CDTIPNO.

To the best of our knowledge, studies of thermodynamic (ΔH_R, ΔS_R) and kinetic ($\Delta H^{\ddagger}_1$, $\Delta S^{\ddagger}_1$, $\Delta H^{\ddagger}_{-1}$, $\Delta S^{\ddagger}_{-1}$) parameters, in the field of nitroxide recognition, have only been reported by Lucarini and co-workers[22] for the bimolecular inclusion of a nitroxide into a calixarene cavity. Although their values strongly differ from ours, the trends found in the noncovalent mode for nitroxide inclusion into calixarene may also hold for the TIPNO in permethylated CD carrier system. Hence, on thermodynamic grounds, the small observed ΔH_R means that the nonassociated **B** form is as stabilized as the weakly associated **A** form. This is likely due to the steric strain of the isopropyl group of the TIPNO moiety overbalancing the stabilizing hydrophobic effect of the methoxy crown.

The non-negligible value of $\Delta H^{\ddagger}_1$ is likely due to steric strain in the transition state because the crown or the cavity must accommodate the nitroxide. In our system, $\Delta H^{\ddagger}_{-1}$ and $\Delta H^{\ddagger}_1$ are very small (the inclusion and exclusion reactions are almost barrierless), meaning that the strain and stabilization in the transition state and in forms A and B are either very similar or match each other. In agreement with the observations of Lucarini and co-workers,[7,22] negative $\Delta S^{\ddagger}$ values were observed, meaning that the transition state is more ordered or "tight" than either the self-included or the open form. Thus, to reach the transition state, the TIPNO moiety must adopt a peculiar conformation (spacer effect). The negative $\Delta S^{\ddagger}_1$ can be due either (i) to the desolvation entropy, (ii) to the approach of the cavity hampered by the crown of methoxy groups, or (iii) to the rigidity of the cyclodextrin backbone (which is unable to modify its conformation for fitting to the nitroxide fragment), although the TIPNO

(57) However, the confidence of this procedure is greatly enhanced if the number of spectra recorded at different temperatures is equal to or greater than 10. See ref 56.

moiety is prepositioned in the space close to the narrow rim of the cavity. On the other hand, the negative $\Delta S^{\ddagger}_{-1}$ is likely due to the spacer effect requiring a peculiar conformation in the transition state of the expulsion reaction.

Finally, kinetic data strongly suggest that the inclusion−exclusion reactions are entropy controlled for the TIPNO−permethyl-β-CD covalent derivative. The thermodynamic values agree with this conclusion, even though interpretation of the results related to ΔS_R must be made with caution. The enthalpic and entropic effects seem to be balanced, involving only a small stability difference between the nonincluded form **B** and the weakly self-included form **A** (i.e., $\Delta G_R > 0$ and $\Delta G^{\ddagger}_{-1} > \Delta G^{\ddagger}_{1}$). The dynamics of the self-association process of **14** is better understood as an exchange between the nonincluded species **B** and the weakly self-included form **A** as depicted in Figure 9.

Conclusion

A TIPNO-type persistent nitroxide has been grafted on a permethylated-β-cyclodextrin, and self-association in water was observed. EPR spectra were simulated assuming a fast exchange between a weakly (loose complex) and a nonassociated species. Competition experiments with methylated β-CDs as external complexing agents revealed that the initial equilibrium was extended by intermolecular complexation of the TIPNO moiety. Simulation of the temperature-dependent EPR spectra with a novel two-dimensional (field-temperature) simulation program afforded thermodynamic and kinetic insights of the self-inclusion process. Several factors influence the binding mode of TIPNO grafted on permethylated-β-CD, among them, the length and flexibility of the spacer arm that appear to be appropriate for nitroxide self-inclusion as well as the shape and polarity of the cavity that is complementary to that of TIPNO. So the binding mode of nitroxide **14** in water can be expressed as a fast exchange between a weakly self-included species **A** and a non-self-included species **B**. In view of these data, the observed changes in the binding modes of **14** with the addition of other CDs are in line with applications of this class of spin-labeled material for the recognition of large supramolecular architectures through nitroxide binding.[13] Finally, this nitroxide represents a good model for further investigations of nitrone-appended cyclodextrins for EPR spin trapping, in terms of the kinds of cyclodextrin, guest, and spacer.

Experimental Section

General. All reactants were used as received without further purification. Crude materials were purified by flash chromatography on silica gel 60 (0.040−0.063 mm). ^{1}H NMR and ^{13}C NMR spectra were recorded at 300.13 and 75.54 MHz, respectively. Melting points were measured on a Büchi B-540 apparatus and are uncorrected. Mono-6-azido-6-deoxy-2,3-di-*O*-methyl hexakis(2,3,6-tri-*O*-methyl)-β-cyclodextrin was kindly provided by Cyclolab R&D (Budapest, Hungary).

2-Hydroxy-1,1-dimethylethyl 2-methyl-1-phenylpropyl nitroxide, TIPNOOH (6b). TIPNOOH was prepared by the procedure of Klaerner et al.[23] with a reaction time of 3.5 h. Flash chromatography: $R_f = 0.3$; pentane/AcOEt, 16/4, 66%, red orange oil; $C_{14}H_{22}NO_2$, $M = 236.33$; EPR (water, 6 lines, $a_N = 1.598$ mT, $a_H = 0.261$ mT); MS (3 mM ammonium acetate in methanol, ESI+) *m/z* 237 $[M + H]^+$, 254 $[M + NH_4]^+$, 259 $[M + Na]^+$, 275 $[M + K]^+$.

2-Succinimidyloxycarbonyloxy-1,1-dimethylethyl 2-methyl-1-phenylpropyl nitroxide, TIPNO-C (11). Triethylamine (1.2 equiv) was added dropwise to a solution of TIPNOOH **6b** (200 mg, 1 equiv) and disuccinimidyl carbonate (304 mg, 1.4 equiv) in acetonitrile (6 mL) under a nitrogen atmosphere. After stirring the mixture for 16 h at room temperature, the solvent was distilled under reduced pressure. The residue was dissolved in methylene chloride (20 mL) and washed with distilled water (8 mL) and with a saturated $NaHCO_3$ solution (8 mL). The organic phase was then washed with brine (8 mL) and dried over Na_2SO_4. Distillation of the solvent under reduced pressure gave the crude product (170 mg) which was used directly in the next step without further purification. $C_{19}H_{25}N_2O_6$, $M = 377.42$; MS (3 mM ammonium acetate in methanol, ESI+) *m/z* 378 $[M + H]^+$, 395 $[M + NH_4]^+$, 400 $[M + Na]^+$, 416 $[M + K]^+$.

2-*N*-Isopropylcarbamoyl-1,1-dimethylethyl 2-methyl-1-phenylpropyl nitroxide (6c). A solution of TIPNO−carbonate **11** (65 mg, 0.17 mmol) and triethylamine (17.5 mg, 0.15 mmol) in dichloromethane (2 mL) was added dropwise to a solution of *iso*-propylamine (31 mg, 0.52 mmol) and triethylamine (17.5 mg, 0.15 mmol) in anhydrous dichloromethane (3 mL) under nitrogen. The solution was then stirred for 50 min and washed with distilled water (10 mL). The organic phase was washed with a saturated aqueous $NaHCO_3$ solution (2 × 10 mL) followed by brine (10 mL) and dried with anhydrous $MgSO_4$. Distillation under reduced pressure yielded an orange oil (41 mg, 85%) which was purified by preparative thin-layer chromatography [eluent CH_2Cl_2/EtOH (95/5)] to afford **6c**. $C_{18}H_{29}N_2O_3$, $M = 321.44$; EPR (water, 6 lines, $a_N = 1.595$ mT, $a_H = 0.267$ mT); MS (3 mM ammonium acetate in methanol, ESI+) *m/z* 322 $[M + H]^+$, 339 $[M + NH_4]^+$, 344 $[M + Na]^+$, 360 $[M + K]^+$.

6-Monoamino-6-monodeoxy-(2,3-di-*O*-methyl)hexakis(2,3,6-tri-*O*-methyl)-β-cyclodextrin hydrochloride (13). 6-Monoamino-6-monodeoxy-TRIMEB-β-CD was prepared by a slight modification of the method of Jicsinszky and co-workers[24] [20 min instead of 10 min heating time and a larger excess of hydrazine hydrate (8 equiv instead of 5 equiv)]: $R_f = 0.20-0.25$ (acetone), 70%, white powder, mp 140−143 °C (lit.[24] 158−161 °C); δ_H 3.17−3.97 (m, 42H), 3.39 (s, 18H), 3.51 (s, 21H), 3.61 (s, 21H), 5.02−5.28 (m, 7H), 8.27 (s, 3H).

2-*N*-6-[-6-Deoxy-2,3-di-*O*-methyl)hexakis(2,3,6-tri-*O*-methyl)-β-cyclodextrinyl]carbamoyl-1,1-dimethylethyl 2-methyl-1-phenylpropyl nitroxide, 236CDTIPNO (14). Under nitrogen, triethylamine (19 μL, 1 equiv) was added to a vigorously stirred solution of monoamino-6-monodeoxy-permethyl-β-CD hydrochloride **13** (200 mg, 1 equiv) in anhydrous dichloromethane (14 mL). A solution of the above-described crude **11** (170 mg) in dichloromethane (8 mL) was then added, followed by a second equivalent of triethylamine. The reaction evolution was followed by TLC. After 1 h, the organic phase was washed with water (10 mL) and with a saturated $NaHCO_3$ solution (10 mL). The organic phase was then washed with brine (10 mL) and dried over Na_2SO_4. After filtration, the solvent was distilled under reduced pressure, and the residue was purified by flash chromatography on silica gel (gradient CH_2Cl_2, 100%; CH_2Cl_2/EtOH 95, 19/1) to afford **14** as a viscous orange oil (180 mg, 78%). $C_{77}H_{131}N_2O_{37}$, $M = 1675.9$; EPR ($CDCl_3$, 6 lines, $a_N = 1.472$ mT, $a_H = 0.264$ mT); MS (3 mM ammonium acetate in methanol, ESI+) *m/z* 1694.0 $[M + NH_4]^+$, 1699.1 $[M + Na]^+$, 1715.0 $[M + K]^+$, 856.2 $[M + 2NH_4]^{2+}$. $C_{77}H_{131}N_2O_{37}$, 2 EtOH, 1.1 CH_2Cl_2 (1676.87 g mol^{-1}) requires C, 54.35; H, 8.07; N, 1.54. Found: C, 54.05; H, 8.37; N, 1.64. Exact mass: calculated for $[C_{77}H_{131}N_2O_{37}]^+Na^+$ 1698.8328. Found 1698.8311.

EPR Measurements. EPR spectra were recorded at room temperature, unless otherwise specified, on a Bruker ESP 300 EPR spectrometer at 9.5 GHz (X-band) employing 100 kHz field modulation and equipped with a Variable Temperature Unit Bruker ER 4111VT. Reaction mixtures were prepared in a chelex-treated phosphate buffer (0.1 M, pH 7.4) with a fixed concentration of nitroxide (5×10^{-4} M) unless otherwise specified. Typical spectrometer settings: microwave power, 10 mW; amplitude modulation, 0.024 mT; time constant, 0.640 ms; receiver gain, 5×10^4; sweep width, 6 mT; sweep time, 84 s. EPR spectra were simulated with two kinds of 2D EPR software: a 2D simulation of the

magnetic field versus concentration[25] and a 2D simulation of the magnetic field versus temperature.[56]

Binding Constant Calculations. EPR titrations were performed at a constant concentration (5×10^{-4} M) of **6a** and **6c** with progressively increasing the amount of cyclodextrin (from 0.05×10^{-3} to 105×10^{-3} M). The samples were prepared by mixing predetermined volumes of freshly made stock solutions of **6a** and **6c** and of TRIMEB, changing progressively the cyclodextrin concentrations and completing, when necessary, with phosphate buffer to reach the desired final concentrations.

Temperature-Dependent EPR Spectra. Two models have been considered for the simulations of the recorded EPR spectra. The first supposes a superimposition of two species in agreement with the diastereoisomeric model (d) of Figure 5. The simulations allowed the determination of the EPR parameters of both species at each temperature. The second way to simulate the EPR spectra supposes a chemical exchange between two species in line with the model (a) of Figure 5, with the rate constants and the populations that can be deduced from the mathematical treatment. In this case, the only limitation is that the program simulating the spectra on a one-by-one basis cannot derive both EPR parameters and the kinetic constants at each temperature. Therefore, the EPR parameters have been fixed for **A** ($a_N = 1.54_3$ mT, $a_H = 0.26_4$ mT, $\Delta H_{pp} = 0.057$ mT) and **B** ($a_N = 1.57_1$ mT, $a_H = 0.25_2$ mT, $\Delta H_{pp} = 0.172$ mT), and the populations and exchange time were adjusted to obtain the best fit. We have to stress that quite different values were derived from the program depending on the preliminary fixed EPR parameters. However, the trend for the calculated k_1, k_{-1}, P_A, P_B, and K values was not affected by the choice of the initial values of a_N, a_H, and ΔH_{pp}, only the scale was shifted, which allows a reliable determination of the kinetics and thermodynamics of the self-inclusion reaction. The better fit obtained by the exchange model compared to the case when only superimposition was assumed strongly suggests a chemical exchange between the A and B species instead of the diastereoisomeric equilibrium.

Acknowledgment. The authors thank the Conseil Régional Provence Alpes Côte d′Azur, the CNRS, the Université de Provence and TROPHOS Company for financial support. Laurence Charles and Valérie Monnier (Spectropole, Universités d′Aix-Marseille I et III), are thanked for the mass spectrometry study of **6c**, **11**, **12**, and **14**. A.R. expresses his thanks for partial financial support of the Hungarian Scientific Research Fund (OTKA T-046953) and the grant NKFP 1/A/005/2004 "MediChem2".

Supporting Information Available: Experimental and calculated spectra for inclusion of **6a** in CD are displayed in Figure 1 of the Supporting Information. This material is available free of charge via the Internet at http://pubs.acs.org.

JO061194P